IEEE Access
Multidisciplinary : Rapid Review : Open Access Journal

Received August 30, 2020, accepted September 9, 2020, date of publication September 18, 2020, date of current version September 30, 2020.

Digital Object Identifier 10.1109/ACCESS.2020.3025222

A Differential Evolution-Based Optimized Fuzzy Logic MPPT Method for Enhancing the Maximum Power Extraction of Proton Exchange Membrane Fuel Cells

MOKHTAR ALY[1,2], (Member, IEEE), AND HEGAZY REZK[3,4]
[1]Department of Electrical Engineering, Aswan University, Aswan 81542, Egypt
[2]Department of Electronics Engineering, Universidad Técnica Federico Santa María, Valparaíso 2390123, Chile
[3]College of Engineering at Wadi Addawaser, Prince Sattam Bin Abdulaziz University, Wadi Addawaser 11991, Saudi Arabia
[4]Department of Electrical Engineering, Faculty of Engineering, Minia University, Minia 61517, Egypt

Corresponding author: Hegazy Rezk (hr.hussien@psau.edu.sa)

This work was supported by the Deanship of Scientific Research at Prince Sattam Bin Abdulaziz University under Project 2020/01/11742.

ABSTRACT Recently, fuel cells (FCs) have found vast employment in several applications. However, unique maximum power point tracking (MPPT) exists for each set of operating condition for the efficient operation of FCs. Therefore, this paper presents a differential evolution optimization algorithm (DEOA)-based optimized fuzzy-logic (OFLC) MPPT method for enhancing the maximum power extraction of FCs. The various settings for the membership functions (MFs) of the input and output variables are optimized in the proposed method. Thence, more degree-of-freedom can be employed for accurate and fast tracking of the optimal power point of the proton exchange membrane FCs (PEMFCs). Whereas, existing MPPT methods in the literature for FC applications suffer from decreased degree-of-freedom for optimizing their performance, and lack of adaptivity, which obstructs their suitability for the wide operating range of FCs. The superiority and performance effectiveness of the proposed OFLC MPPT method have been validated and compared with the most prevalent techniques in the literature. Moreover, the robustness and sensitivity of the proposed OFLC MPPT method have been tested at various step changes in the water content of membrane and various temperature changes. Moreover, the proposed design of the suggested OFLC MPPT is general and it can be implemented on low-cost microcontrollers. The results verify the superior performance of the proposed OFLC MPPT method from the accurate and fast MPPT extraction, smooth output power with low ripple, and simplicity of the design point of views.

INDEX TERMS Differential evolution optimization algorithm (DEOA), fuel cell (FC), fuzzy logic control (FLC), maximum power point tracking.

I. INTRODUCTION

Global warming and limited existence of fossil fuels have directed governments to put their ambitious plans of green energy technologies. Renewable energy environmentally-friendly sources have proven efficient, clean, and low cost candidates to the traditional fossil fuels [1]–[5]. Several studies have been performed for evaluating the joint technical-economical long term impacts of RESs installations [6], [7]. In addition, the continual cost decrease of the RES technologies and parts have lead to intensive widespread world-widely. However, the stochastic behavior of RESs and/or their connected electrical loads has given rise to energy supply reliability issues. Therefore, installations of energy storage systems (ESSs) with the RESs increase their power supply reliability and improve their techno-economical issues for long-term operation [8], [9]. The selection, sizing, and control of various existing ESS are crucial factors for wide installation of RESs [10].

Among the various existing ESS, battery ESSs have been widely employed with RESs in wide range of electrical power installations. However, the short operating lifetime and increased replacement costs represent the main critical issues for battery ESSs [11], [12]. Another alternative

The associate editor coordinating the review of this manuscript and approving it for publication was Pengcheng Liu.

is through converting the excess electrical power from the RES into hydrogen via employing electrolyzers. Afterwards, the generated hydrogen is stored and utilized as source for powering fuel cells (FCs) ESSs [13], [14]. The FC technology is an electrochemical device, which combines the hydrogen and oxygen for generating electricity. The main advantages of FCs to be comparable alternatives to existing ESSs are possessing high reliability and efficiency, being noise-free ESSs, and eliminating pollution from environment. There are several types and technologies of FCs, such as the alkaline FC, molten carbonate FC, proton exchange membrane FC (PEMFCs), direct methanol FC, phosphoric acid FC, and solid oxide FC. Among them, PEMFCs are light-weight, fast starting-up, low operation temperature, and high power density FC solutions. Thence, PEMFCs represent the most popular utilized type of FCs, in addition to being high performance candidates for vehicular and residential RES applications [15], [16].

The characteristics of FCs output exhibits nonlinear behavior and they are influenced by several factors, including the operating temperature, and the water contents of membrane [17]. However, the output current-power curves of the PEMFCs have unique maximum power point (MPP) for every particular operating condition. Thence, finding the optimum operating point of FC voltage and/or current is important for maximizing the energy utilization and efficiency of PEMFCs. Particularly, the MPP can be achieved through continual MPP tracking (MPPT) of the PEMFC [18]. In [19], the performance of using MPPT for FC applications have been compared to without MPPT operation. There are several methods have been proposed in the literature for MPPT of FCs. The MPPT controllers set the operating duty cycle of the FC interfacing dc/dc converter at the MPP operation. The main performance criteria to compare the various MPPT methods are the speed of tracking, the ripple and fluctuation of FC power, the computational burdens, the implementation complexity, and the required number of sensors.

The perturb and observe (P&O) MPPT method has been widely applied in the literature for controlling PEMFCs. A P&O MPPT method with the static, and dynamic modeling of PEMFCs has been presented in [20]. The incremental conductance (INC) and the incremental resistance (INR) MPPT methods have proven better transient and steady state performance compared to the P&O method [21]. In [22], the P&O and INC MPPT methods have been applied with boost dc/dc converter for FC-supplied electric vehicles (EVs). Another application of the P&O method with high stepping-up ratio dc/dc converter has been introduced in [23]. The variable step size INR and variable step size INC methods have been proposed for improving the performance of PEMFCs [24]. Another fractional order (FO) INC method has been presented in [25] with wide range variable step size controlling of the MPPT. Moreover, artificial neural network (ANN) based variable step size INC MPPT method has been presented for enhancing the outputted power of FCs in [26]. The JAYA optimization has been proposed for controlling MPPT for hybrid photovoltaic (PV)/FC/ultra-capacitor grid tied systems in [27].

Additionally, two cascaded loops control methods with intermediate dc/dc power converter have been presented for FC MPPT in the literature [28]. The outer control loop determines the real-time MPP operating point through using extremum seeking algorithms. This stage defines the MPPT reference voltage for the inner loop, which controls the power conversion stage to the desired reference set-point. The widely-employed proportional-integral-derivative (PID) controllers are used in the inner loop, wherein their tuning process is critical issue for maximizing the efficiency of PEMFCs. The salp swarm algorithm (SSA) has been proposed in [29] for optimizing the PID controller parameters. The grey wolf optimizer (GWO) has been presented in [30] for extracting the MPP of PEMFC at variable operating conditions. In addition, the particle swarm optimization (PSO) method has been also provided for designing the PID controller in [28]. Whereas, the sine cosine algorithm (SCA) method has been applied with PID controllers in [31]. The antlion optimizer (ALO) method was presented in the literature for designing the MPPT PID controller in [32]. The various performance criteria between these optimization methods has been performed in [21].

From another side, fuzzy logic control (FLC) methods provide single loop MPPT controllers with high operating performance [33]. The design of FLC MPPT for FC applications has been presented in [34]. An INC-based FLC MPPT method has been introduced in [35]. This approach simulates the incorporated MPPT control for PV/FC hybrid systems through controlling the buck dc/dc converter. The performance comparison of the Mamdani and Sugeno types of the FLC MPPT has been provided in [36]. The design of the asymmetrical membership function (MF) of the FLC-based MPPT method has been introduced using the firefly approach in [37]. The Mamdani type FLC MPPT method has been presented in [38], and its performance was compared to the PSO-based MPPT method. Additional optimization methods have been proposed in the literature for enhancing the MPPT performance in several applications [39]–[41]. Several hybrid optimization algorithms-FLC methods have been proposed in the literature for PV applications [42]–[44]. Moreover, several ANN based MPPT method have been presented in the literature [26]. The adaptive neuro-fuzzy inference system (ANFIS) based MPPT has been presented for PEMFCs in [45]–[48]. Another ANFIS based MPPT method has been presented for EVs applications [49]. In addition, the neural network based MPPT algorithms have been proposed for controlling PEMFCs [50].

However, the performance parameters of the existing controllers have several challenges regarding the tracking time, the steady state performance, implementation complexity, the real-time applicability, and the sensors cost. Meanwhile, achieving optimized performance is highly dependant on the degree of freedom of the employed MPPT technique. Apart from that, the FLC methods provide multiple degree-of-freedom in their design in selecting their MFs, the boundaries of both input and output MFs, and the shapes and locations of points in their MFs. The presented FLC-based MPPT solutions in the literature employ fixed design points by trial and error. Therefore, this paper is presenting an optimized FLC (OFLC) MPPT method for PEMFCs. The main contribution in this paper can be summarized as follows:

- A new optimized FLC (OFLC) MPPT method is proposed for controlling PEMFCs. The proposed design enables the utilization of the high degree-of-freedom in the FLC methods.
- The high performance Differential Evolution Optimization Algorithm (DEOA) is applied in this paper for optimizing the design process of OFLC MPPT controllers.
- The OFLC MPPT has been designed and validated through comprehensive comparisons with the featured MPPT techniques in the literature for PEMFCs.
- An improved optimum power extraction with fast tracking performance for PEMFCs is introduced through the proposed OFLC MPPT design.

The remaining of the paper is organized as following: Section II presents the modeling and behavior of PEMFCs. The FLC MPPT control of PEMFCs in introduced in Section III. Section IV details the new proposed OFLC and the PSO optimization method. Section V provides the main results and comparison of the performance of the proposed OFLC MPPT method with the existing methods in the literature. The discussion and superior features of the proposed OFLC MPPT are presented in Section VI. Finally, The paper is concluded in Section VII.

II. MODELING AND CHARACTERISTICS OF PEMFC

This section provides the dynamic modeling of PEMFC and their main characterstics are introduced. The mathematical model and the various factors that affect their performance are presented, including Nernst voltage component, in addition to the activation, concentration, and the ohmic losses.

A. DYNAMIC MODEL OF GAS TRANSPORT

The gas flow through the valve of FC is related to the partial pressures of both the hydrogen, and the oxygen as follows for the hydrogen [28]:

$$\frac{q_{H_2}}{P_{H_2}} = \frac{k_{an}}{\sqrt{M_{H_2}}} = K_{H_2} \tag{1}$$

And, for the oxygen is expressed as follows [21]:

$$\frac{q_{O_2}}{P_{O_2}} = \frac{k_{an}}{\sqrt{M_{O_2}}} = K_{O_2} \tag{2}$$

where, q_{O_2} and q_{H_2} denote to the molar flow for the oxygen, and hydrogen, respectively, and K_{O_2} and K_{H_2} are their corresponding molar constants (kmol (atm s)$^{-1}$). Whereas, P_{O_2} and P_{H_2} represent the partial pressure for the oxygen and the hydrogen (atm), respectively. In addition, k_{an} represents the anode valve constant, and M_{O_2} and M_{H_2} are the oxygen and hydrogen molar masses. The derivative of partial pressure is calculated using perfect gas formulation as follows [21]:

$$\frac{dP_{H_2}}{dt} = \frac{RT}{V_{an}}(q_{H_2}^{in} - q_{H_2}^{out} - q_{H_2}^{r}) \tag{3}$$

$$\frac{dP_{O_2}}{dt} = \frac{RT}{V_{an}}(q_{O_2}^{in} - q_{O_2}^{out} - q_{O_2}^{r}) \tag{4}$$

where, R denotes to the universal gas constant, T represents the temperature (in Kelvin), and V_{an} represents the anode volume. Whereas, $q_{H_2}^{in}$ and $q_{H_2}^{out}$ denote to the input and output flow rates for the hydrogen, respectively. Also, $q_{O_2}^{in}$ and $q_{O_2}^{out}$ denote to the input and output flow rates for the oxygen, respectively. In addition, $q_{H_2}^{r}$, and $q_{O_2}^{r}$ are the flow rate for the reacted hydrogen and oxygen, respectively, and they can be calculated using the following:

$$q_{H_2}^{r} = q_{O_2}^{r} = \frac{N_{FC} I_{FC}}{2F} = 2k_r I_{FC} \tag{5}$$

where, N_{FC} represents the number of series connected FCs, I_{FC} represents the output current of the FC, F denotes to Faraday's constant, and k_r represents constant of the modeling. The instantaneous partial pressures for the hydrogen and oxygen can be obtained by solving (1) and (2) as following for the hydrogen:

$$P_{H_2}(t) = \frac{1}{k_{H_2}}(2k_r I_{FC} e^{(-t/\tau_{H_2})} + q_{H_2}^{in} - 2k_r I_{FC}) \tag{6}$$

where,

$$\tau_{H_2} = \frac{V_{an}}{k_{H_2} RT} \tag{7}$$

Similarly, the partial pressure for the oxygen is derived as following:

$$P_{O_2}(t) = \frac{1}{k_{O_2}}(2k_r I_{FC} e^{(-t/\tau_{O_2})} + q_{O_2}^{in} - 2k_r I_{FC}) \tag{8}$$

where

$$\tau_{O_2} = \frac{V_{an}}{k_{O_2} RT} \tag{9}$$

The relationship among the FC current I_{FC} and the partial pressure of the hydrogen is described using (6). Whereas (8) describes the relationship among FC current I_{FC} and the partial pressure of the oxygen.

B. MODEL OF POLARIZATION CURVE

In PEMFCs, there are three main components of power losses, including the activation V_{act}, the ohmic V_{ohm}, and the concentration V_{con} losses. The terminal voltage of the FC stack V_{FC} can be estimated as following:

$$V_{FC} = N_{FC} \times V_{cell} = N_{FC} \times (E_{Nernest} - V_{act} - V_{ohm} - V_{con}) \tag{10}$$

where $E_{Nernest}$ is the Nernest voltage of the FC and it can be modelled as follows:

$$E_{Nernest} = 1.229 - 8.5 \times 10^{-4}(T - 298.15) + 4.385 \times 10^{-5} T(\ln P_{H_2} + 0.5 \ln P_{O_2}) \tag{11}$$

The activation loss of the FC can be expressed based on the model in [28] as follows:

$$V_{\mathrm{act}} = -[\xi_1 + \xi_2 T + \xi_3 T \ln(C_{O_2}) + \xi_4 T \ln(I_{\mathrm{FC}})] \quad (12)$$

where, $\xi_1, \xi_2, \xi_3, \xi_4$ are the parametric coefficients. They can be obtained through curve fitting using modern optimization techniques as in [29]. In addition, the selected case study is based on the data provided in [28]. Whereas C_{O_2} represents the concentration of dissolved oxygen at gas/liquid interface, and it can expressed as following:

$$C_{O_2} = \frac{P_{O_2}}{(5.08 \times 10^6) \times \exp(-498/T)} \quad (13)$$

From another side, the ohmic loss V_{ohm} is generated due to the membrane resistance R_{m}. It can be estimated as following:

$$V_{\mathrm{ohm}} = I_{\mathrm{FC}} R_{\mathrm{m}} \quad (14)$$

where, R_{m} is estimated as following:

$$R_{\mathrm{m}} = \frac{r_{\mathrm{m}} l}{A} \quad (15)$$

where, r_{m} represents the resistivity of the membrane to the proton conductivity, l represents the thickness of the membrane, and A denotes to the FC active area. The membrane resistivity r_{m} is strongly dependant on humidity and temperature of the membrane and it can be estimated as following [21]:

$$r_{\mathrm{m}} = \frac{181.8[1 + 0.03(\frac{I_{\mathrm{FC}}}{A}) + 0.0062(\frac{T}{303})(\frac{I_{\mathrm{FC}}}{A})^{2.5})]}{[\lambda_{\mathrm{m}} - 0.634 - 3(\frac{I_{\mathrm{FC}}}{A}) \exp(4.18\frac{T-303}{T})]} \quad (16)$$

where, λ_{m} represents the water content of the membrane. The concentration loss V_{con} is generated via the consumption of concentration gradient of the reactants, and it is estimated as following:

$$V_{\mathrm{con}} = \frac{RT}{nF} \ln(1 - \frac{I_{\mathrm{FC}}}{I_{\max} A}) \quad (17)$$

where, n represents the number of the participated electrons during the reaction, and $I_{\max}$ denotes to the maximum limiting current. It represents the maximum rate for the reactant to be supplied to the electrode, and it is usually defined by the manufacturer datasheet [51]. Finally, the total generated power from the FC stack P_{FC} can be represented as follows:

$$P_{\mathrm{FC}} = V_{\mathrm{FC}} I_{\mathrm{FC}} \quad (18)$$

C. CHARACTERISTICS OF PEMFC

The aforementioned mathematical modeling of PEMFCs is programmed using Matlab environment. The various characterstics have been tested at the various operating conditions. Firstly, the PEMFC outputted power-current and outputted voltage current curves are plotted at various operating temperatures and constant water content ($\lambda_{\mathrm{m}} = 12$) in Fig. 1. Moreover, Fig. 2 shows performance characterstics of PEMFC output at different water contents and constant temperature $T = 343\ K$. The characteristic curves confirm the necessity of MPPT for PEMFCs operation due to their nonlinear behavior and they exhibits unique MPP operation. Thence, the tracking method is crucial at determining the efficiency and outputted power of the PEMFC.

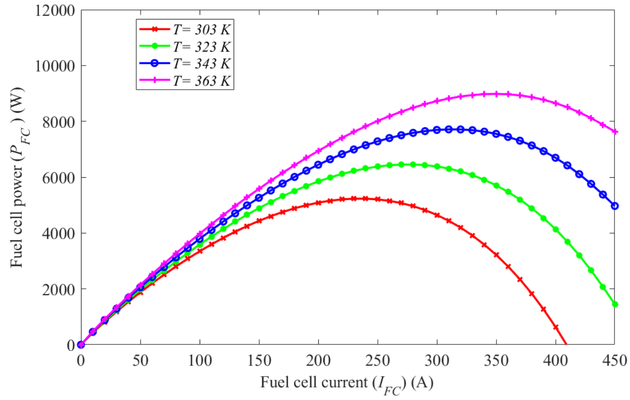

(a) Fuel cell output power-current curves

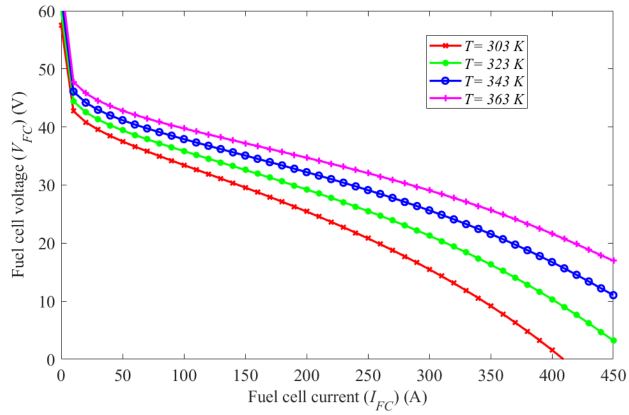

(b) Fuel cell output voltage-current curves.

FIGURE 1. The performance characterstics of PEMFC output at different temperatures and constant water content ($\lambda_{\mathrm{m}} = 12$).

D. FUEL CELL ELECTRICAL SYSTEM

It has become clear that PEMFCs have unique operating MPPT, which has to be continually tracked so as to maximize the FC efficiency. The main influencing factors for the operating MPP are the temperature and the water content of the membrane. The MPP is determined mainly through the slope of the P_{FC}-I_{FC} curve and the slope of the V_{FC}-I_{FC}. A dc/dc power conversion stage is usually employed to perform the MPPT control action and set the operating point of the FC at the determined MPPT by the algorithm. Fig. 3 shows the electrical system of the PEMFC with using boost dc/dc converter. The boost dc/dc converter is operated at the continuous conduction mode (CCM) for efficient power conversion and continuous input current from the PEMFC source. The output voltage of the boost dc/dc converter is a step-up from the low input voltage of the PEMFC and the step-up ratio is determined by the duty cycle D of the converter [33]. The output voltage V_{out} and input voltage V_{in}

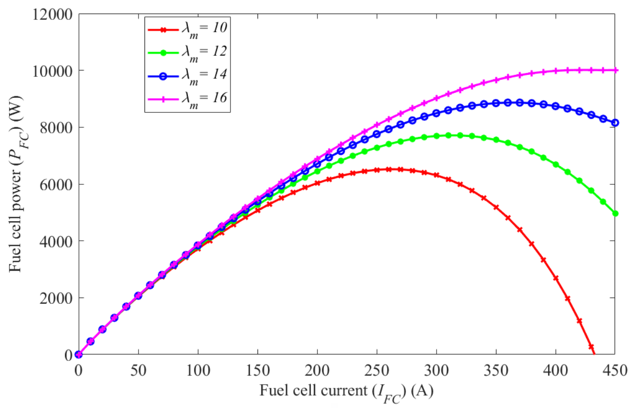

(a) Fuel cell output power-current curves

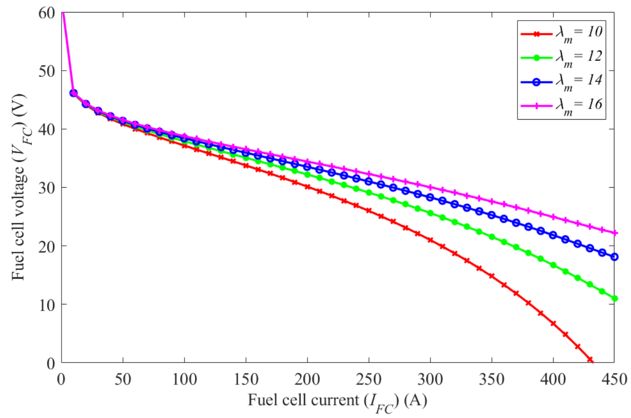

(b) Fuel cell output voltage-current curves

FIGURE 2. The performance characterstics of PEMFC output at different water contents and constant temperature $T = 343$ K.

are related as following:

$$\frac{V_{\text{out}}}{V_{\text{in}}} = \frac{1}{1-D} \tag{19}$$

III. FLC BASED MPPT OF PEMFC

The FLC has found wide application in MPPT for PV systems, wherein enhanced performance is achieved over classical methods [33]. Fig. 4 shows the main stages of FLC systems, which include the fuzzification stage, the fuzzy inference engine, and the defuzzification stage. In the stage of fuzzification, crisp inputs variables are converted to linguistic labels according to the predefined input MFs. The converted linguistics labels in the first stage are employed as fuzzy input to generate verbal decisions. The fuzzy inputs are utilized by the fuzzy inference engine based on the ''if-then rules'' concept to generate the fuzzy output. In the third stage, the generated fuzzy outputs are converted to crisp values [52]. For MPPT applications of FLC systems, two inputs are utilized to generate one output to operate the system at the MPP. The input variables can be defined as follows:

$$E(k) = \frac{dP_{\text{FC}}}{dV_{\text{FC}}} = \frac{P_{\text{FC}}(k) - P_{\text{FC}}(k-1)}{V_{\text{FC}}(k) - V_{\text{FC}}(k-1)} \tag{20}$$

$$\Delta E(k) = E(k) - E(k-1) \tag{21}$$

where $E(k)$ represents the error signal of the change in the slope of the P_{FC}-V_{FC} curve at the current time instant (k), $\Delta E(k)$ denotes to the change in the error signal between the $(k)^{\text{th}}$ and the $(k+1)^{\text{th}}$ time instants, $P_{\text{FC}}(k)$ and $V_{\text{FC}}(k)$ represent the sampled FC power and voltage signals at the time instant (k), respectively, and the $P_{\text{FC}}(k-1)$ and $V-\text{FC}(k-1)$ represent their sampled signals at the time instant $(k-1)$. Whereas, the output variable is the increment/decrements duty cycle $\Delta D(k)$, which is employed with the duty cycle from the previous time step to generate the current operating duty cycle. Fig. 5 shows the main structure for the input and output signals and the main components of the FLC MPPT methods. The output duty cycle for the MPPT, which is applied to the boost dc/dc converter can be expressed as following:

$$D(k) = \Delta D(k) + D(k-1) \tag{22}$$

The waveforms of the input variables and the output variable for FLC MPPT systems are shown in Fig. 6. In each variable, there are seven MFs to represent the input and output variables, including three positive levels (Pos_L3, Pos_L2, and Pos_L1), one zero level (Zer_L0, and three negative levels (Neg_L3, Neg_L2, and Neg_L1).

IV. THE PROPOSED OFLC MPPT METHOD

A. CHALLENGES, OBJECTIVES, AND CONTRIBUTIONS

It can be seen from Section II that PEMFCs exhibit nonlinear characteristics, and their performance is dependent on the operating conditions of membrane water content and temperature. Fig. 1 and Fig. 2 show that a unique MPP exists for each particular operating combination of temperature and membrane water content. Therefore, the main objective of this paper is to improve the power extraction of PEMFCs through proposing a new DEOA-based OFLC MPPT method. The main general objectives regarding the performance improvement of PEMFCs are summarized as follows:

- The outputted power from the PEMFC is maximized through the application of the proposed OFLC MPPT method. This in turn enhances the energy efficiency of using PEMFCs in renewable energy applications.
- The tracking performance with the continuously changing operating point is improved through utilizing the proposed fast OFLC MPPT method. This in turn improves the dynamic performance of the PEMFC system in large-scale utility grid integration.

Additionally, the main superiorities of the proposed DEOA-based OFLC MPPT method over the challenges of the existing MPPT methods can be summarized as follows:

- Compared to the widely employed fixed step size MPPT methods, such as P&O and hill climbing MPPT methods, the proposed OFLC MPPT method employs a variable step size MPPT tracking, which provides faster tracking during transients and lower ripples at steady state conditions.

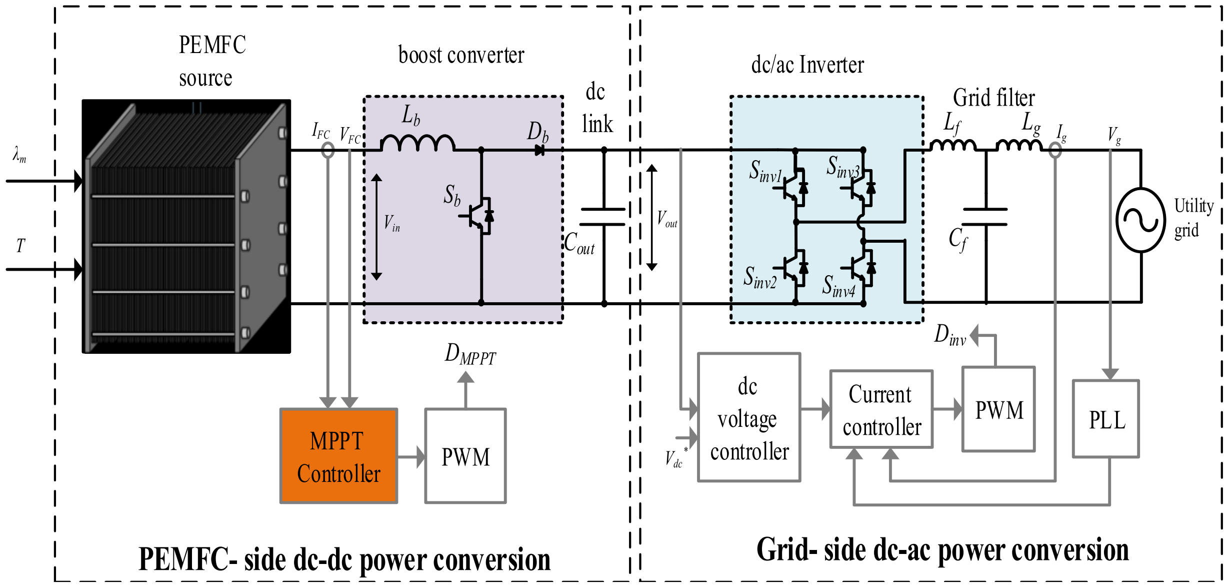

FIGURE 3. The electrical system of grid-tied PEMFC with boost dc/dc converter.

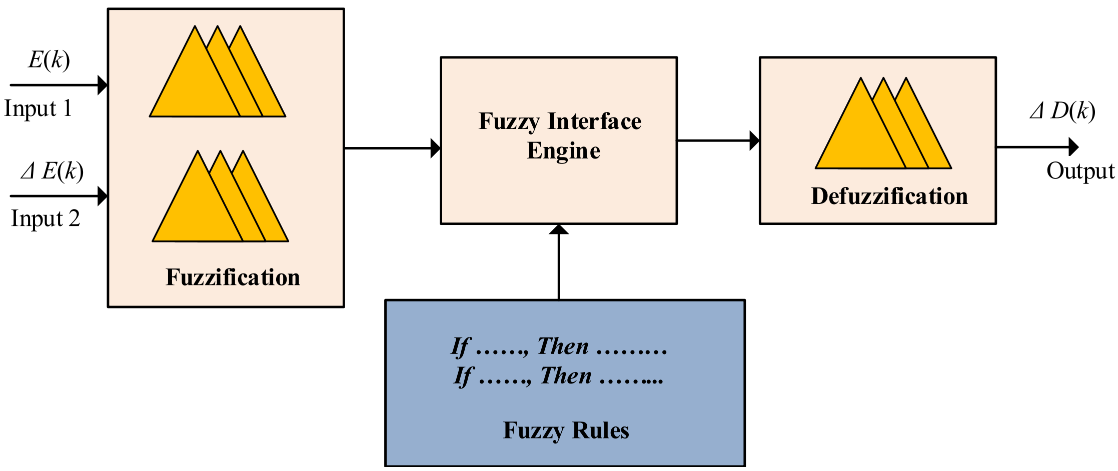

FIGURE 4. The various stages of the FLC-based MPPT method.

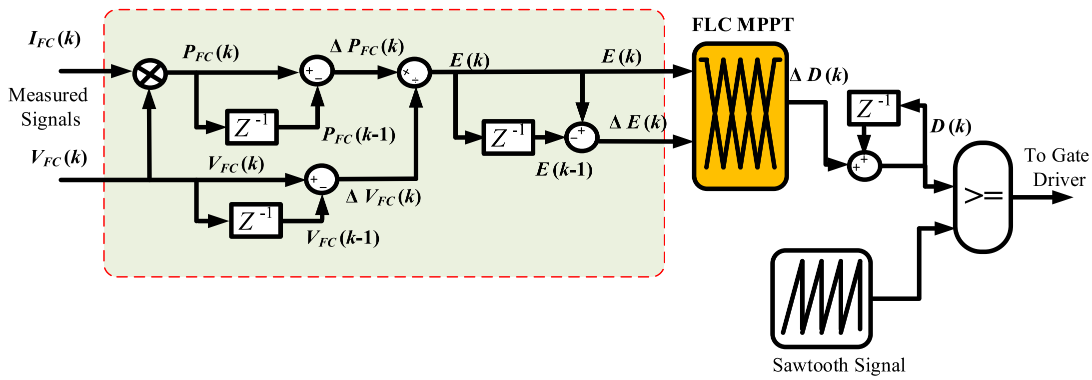

FIGURE 5. The structure and main components in the FLC MPPT control method.

- Compared to existing variable step size MPPT methods such as INC and INR methods, a more adaptive method with faster tracking of MPP is proposed in this paper due to benefiting the inherent adaptivity of FLC systems.
- Compared to neural network, learning-based algorithms, and optimization searching methods, the proposed method represents a more simple and efficient solution without complex procedures, and large training data.

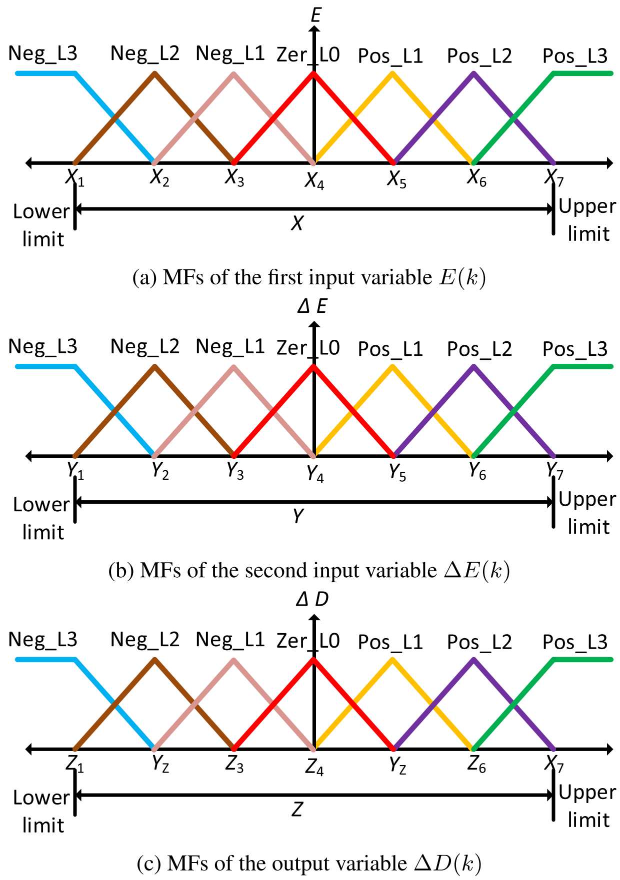

(a) MFs of the first input variable $E(k)$

(b) MFs of the second input variable $\Delta E(k)$

(c) MFs of the output variable $\Delta D(k)$

FIGURE 6. The various MFs of the input and output variables of the FLC MPPT control system.

- Moreover, the performance parameters of the existing controllers have several challenges regarding the tracking time, the steady state performance, implementation complexity, the real-time applicability, and the sensors cost.

From another side, the main contributions and improvements over the existing FLC MPPT methods can be summarized as follows:

- The proposed method employs the efficient DEOA method for optimizing the design of FLC based MPPT methods.
- The proposed design method benefits the employment of the inherent high degree-of-freedom in the FLC systems through optimizing the various parameters of the input and output variables and MFs.
- The optimization process in the proposed method includes multiple degree-of-freedom at optimizing the scaling factors of the input and output variables in addition to the various internal points of the MFs, which determine the shape of MFs. The existing FLC-based MPPT solutions in the literature employ fixed design points, which are usually determined by trial and error adjustment.

The structure and operating principle of the proposed DEOA-based OFLC MPPT method are shown in Fig. 7.

B. THE MFs OF INPUT AND OUTPUT VARIABLES

The proposed optimized FLC method enables benefiting the high degree-of-freedom in the FLC method through optimizing their MFs and their scaling factors. Fig. 8a shows the degree-of-freedom in one of the input variables as a case study of the error $E(k)$ variable. The various points of the MFs ($X_1 \sim X_7$) are optimized in the proposed OFLC MPPT method using the DEOA method. This in turn provides high degree-of-freedom in designing the FLC so as to achieve optimized objective function. Fig. 8b shows a case study of asymmetrical MFs with optimized points. Whereas, Fig. 8c shows another example of optimizing the MF with scaling the lower and upper limits in addition to the shape of the MFs.

C. THE FUZZY RULES

In this step, the fuzzy rules are designed to manage the operation and decisions of the MPPT controller output. In the proposed OFLC MPPT method, there are 7 MFs in each of the two inputs and the output variables. The 7 MFs of each input and output variable has three positive levels (Pos_L3, Pos_L2, and Pos_L1), one zero level (Zer_L0), and three negative levels (Neg_L3, Neg_L2, and Neg_L1). Therefore, there will be 49 rules. Table 1 shows the various rules of the designed OFLC MPPT method.

D. THE OBJECTIVE FUNCTION

The main objective of the tuning of the various elements of the FLC in the proposed OFLC MPPT method is to reach the MPP with fast tracking speed. Therefore, the MFs of the input variables in addition to the output duty cycle have to be optimally determined. The cost function is estimated based on the integral square error (ISE) criteria are used for the cost function [53], which can be expressed as following:

$$ISE = \int_{t=o}^{T_{\text{sim}}} (\Delta E(k))^2 \tag{23}$$

where T_{sim} denotes to the simulation time for evaluating the objective function. The main goal of the optimizer is to determine combinations of optimized variables that achieve the minimized cost function (the error signal) over the simulation time. The well-known min-max based FLC method is applied. In addition, the defuzzification is made through the centroid of area method.

E. DIFFERENTIAL EVOLUTION OPTIMIZATION ALGORITHM (DEOA)

The DEOA is one of the popular algorithms, which is used to solve different optimization problems. DEOA begins the optimization procedures by an arbitrary population. Then, it adjusts the population through the process of optimization; mutation, crossover, and selection. The mathematical representation and physical definition can be found in [54]. In the mutation and crossover phases, a trial vector for every target vector is generated. Next, a selection phase is done between trial and target vectors. The optimization process of DEOA can be summarized by the following; the gains

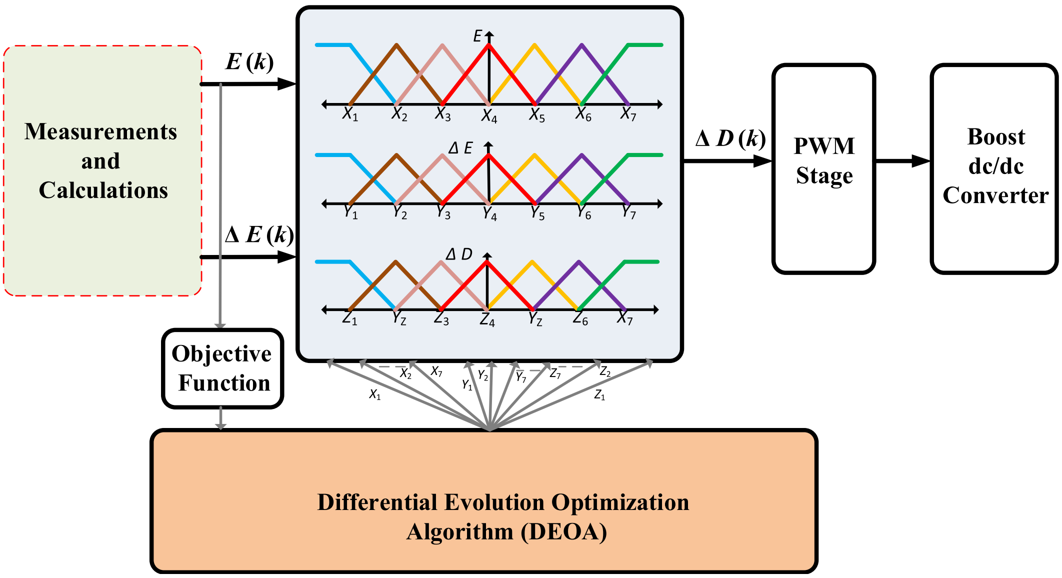

FIGURE 7. The proposed DEOA-based OFLC MPPT method.

TABLE 1. The rules of the proposed OFLC MPPT method between MFs of the input and output variables.

	Input MFs	ΔE						
		Neg_L3	Neg_L2	Neg_L1	Zer_L0	Pos_L1	Pos_L2	Pos_L3
	Neg_L3	Neg_L3	Neg_L3	Neg_L3	Neg_L3	Neg_L2	Neg_L1	Zer_L0
	Neg_L2	Neg_L3	Neg_L3	Neg_L3	Neg_L2	Neg_L1	Zer_L0	Pos_L1
	Neg_L1	Neg_L3	Neg_L3	Neg_L2	Neg_L1	Zer_L0	Pos_L1	Pos_L2
E	Zer_L0	Neg_L3	Neg_L2	Neg_L1	Zer_L0	Pos_L1	Pos_L2	Pos_L3
	Pos_L1	Neg_L2	Neg_L1	Zer_L0	Pos_L1	Pos_L2	Pos_L3	Pos_L3
	Pos_L2	Neg_L1	Zer_L0	Pos_L1	Pos_L2	Pos_L3	Pos_L3	Pos_L3
	Pos_L3	Zer_L0	Pos_L1	Pos_L2	Pos_L3	Pos_L3	Pos_L3	Pos_L3

of fuzzy membership functions are used as a target vector and the error signal as a cost function. The target vectors are arbitrarily located in the range of upper and lower bounds. Next, the created population of gains of fuzzy membership functions are applied to fuel cell system. After that, the error signal is estimated. After the initialization phase is finished, the minimum error value is nominated as best value and the corresponding membership gains are stored as the best one. Then, two different population are randomly nominated. A mutation factor F is used to weight the difference between the selected target vectors. Then, the weighted difference is added to the best membership gains to create donor vector. The mutation phase, which creates the donor vector, can be formulated as following [54];

$$xv_{\mathrm{i}} = x_{\mathrm{best}} + F \times (x_{\mathrm{r_1}} - x_{\mathrm{r_2}}) \tag{24}$$

Where indexes r_1 and r_2 denote two different integers and F denotes a scale factor. Then, the following relation can be used to check if the created element is situated in the determined range.

$$xv_{\mathrm{i}} = \begin{cases} x_{\max}\,, & \text{If } xv_{\mathrm{i}} \text{ greater than } x_{\max} \\ x_{\min}\,, & \text{If } xv_{\mathrm{i}} \text{ lower than } x_{\min} \end{cases} \tag{25}$$

Then, the crossover phase is done to create the trail vector using the nest relation;

$$xv_{\mathrm{i}} = \begin{cases} x_{\mathrm{v_i}}\,, & \text{If } rand \le C_{\mathrm{r}} \\ x_{\mathrm{i}}\,, & \text{otherwise} \end{cases} \tag{26}$$

where, C_{r} is the crossover control parameter. The last phase in the DEOA is the selection phase. The target and trial vectors are compared in this phase. Every trial vector is assessed using fuel cell system and corresponding error signal is estimated. Based on the comparison, the membership gains that corresponds to minimum error signal is used as the next target vector;

$$x_{\mathrm{i+1}} = \begin{cases} xu_{\mathrm{i}}\,, & \text{If } f(xu_{\mathrm{i}}) \le f(x_{\mathrm{i}}) \\ x_{\mathrm{i}}\,, & \text{otherwise} \end{cases} \tag{27}$$

The optimization procedure remains running till an end condition is happened.

V. RESULTS

Table 2 shows the main specifications for the PEMFC for the selected case study based on the specifications provided in [28]. The tested system has the PEMFC as input source, boost converter operated at 20 kHz switching frequency with boost inductor of 0.5 mH and output capacitor of 500 μF.

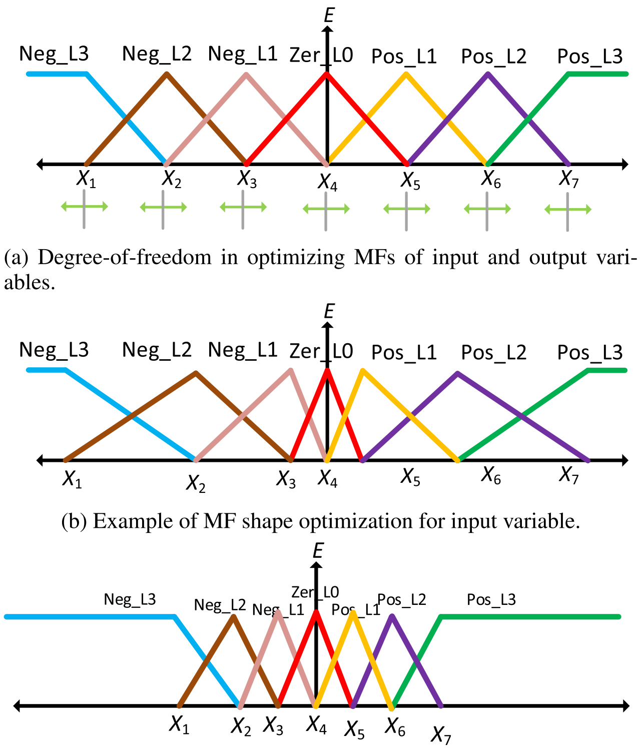

(a) Degree-of-freedom in optimizing MFs of input and output variables.

(b) Example of MF shape optimization for input variable.

(c) Example of scaling factors optimization for input variable.

FIGURE 8. The degree-of-freedom of MFs for the proposed OFLC MPPT method.

TABLE 2. The PEMFC parameters for the selected case study.

Parameter	Value
T	343 (K)
A	232 (cm^2)
l	0.0178 (cm)
N_{FC}	35
I_{max}	2.00 (A cm^{-2})
n	2
F	96484600 (C (kmol^{-1})
R	8.31447 (J (mol K)$^{-1}$)
k_r	9.07×10^{-8} (J (mol K)$^{-1}$)
k_{O_2}	2.11×10^{-5} (kmol (atom S)$^{-1}$)
k_{H_2}	4.22×10^{-5} (kmol (atom S)$^{-1}$)
$q_{H_2}^{in}$	10×10^{-5} (kmol (S)$^{-1}$)
$q_{O_2}^{in}$	5×10^{-5} (kmol (S)$^{-1}$)
ξ_1	0.944
ξ_2	0.00354
ξ_3	7.8×10^{-8}
ξ_4	-1.96×10^{-4}

The PEMFC system has been tested at three different case studies (Case 1 at the normal starting operation, Case 2 at changing membrane water content and fixed temperature, and Case 3 at changing temperature and constant membrane water content).

A. CASE 1: NORMAL STARTING OPERATION

The proposed OFLC MPPT method is tested at the normal starting operation and it is compared to the classical P&O, the INC, and the traditional FLC MPPT method. Fig. 9 shows

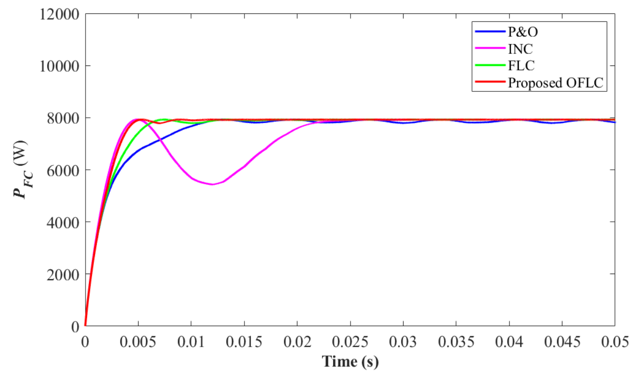

FIGURE 9. The normal starting response of the fuel cell output power for case 1.

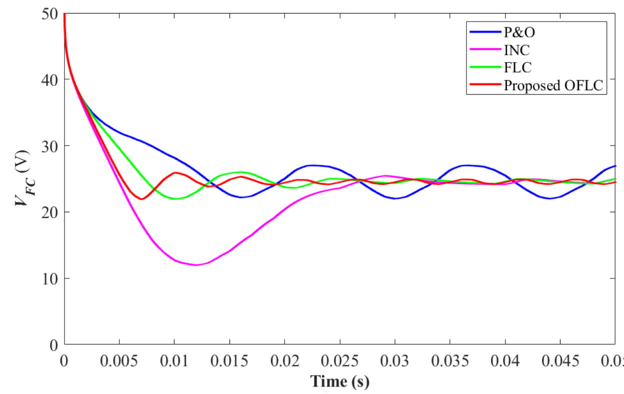

FIGURE 10. The normal starting response of the fuel cell output voltage for case 1.

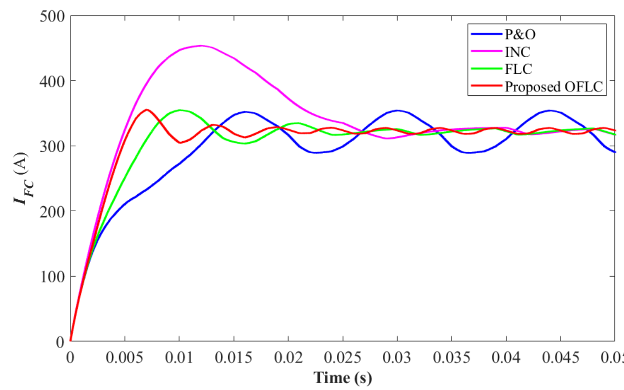

FIGURE 11. The normal starting response of the fuel cell output current for case 1.

the response of the outputted power from the PEMFC at the four considered MPPT methods. It can be seen that the proposed OFLC MPPT method is successful at achieving the fastest tracking of the operating MPPT of the PEMFC. The P&O and INC represent the slowest MPPT algorithms. The INC MPPT method possesses the largest transient time. However, the classical FLC MPPT method has better normal starting performance than the P&O and INC methods. Whereas, optimizing the FLC MPPT in the proposed OFLC method improves its tracking performance over the traditional MPPT methods.

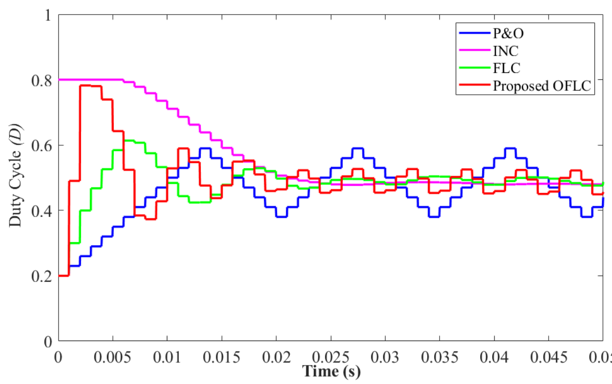

FIGURE 12. Comparison of the output duty cycle *D* at normal starting response for case 1.

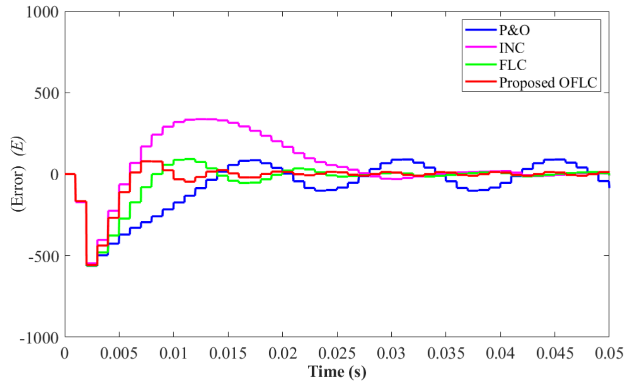

FIGURE 13. Comparison of the error *E* at the normal starting response for case 1.

Fig. 10 shows the output voltage response of the PEMFC for the considered four MPPT methods. The proposed OFLC MPPT method possesses the lowest voltage fluctuations. Whereas, the INC and the P&O have the worst voltage response. Similarly, the PEMFC output current performance is compared in Fig. 11 for the considered MPPT methods. The INC method has higher output current overshoot, which may lead to shortening the operating lifetime of the PEMFC. Whereas, the proposed OFLC and classical FLC MPPT methods achieve better output current performance, which enhances the operating lifetime of the PEMFC. Thence, the proposed OFLC MPPT method provides enhanced starting waveforms of output voltage and current of the PEMFCs.

The outputted duty cycles of the four MPPT methods are compared in Fig. 12. The P&O has fixed step size, which leads to slower response of the MPPT. Whereas, the proposed OFLC MPPT is advantageous due to employing the adaptiveness of the FLC method to achieve better dynamic response. The error signals of the considered MPPT methods are shown in Fig. 13. It can be seen that the proposed OFLC MPPT method minimizes the objective function of the error signal compared to the other existing MPPT methods. The minimized objective function enhances the operating efficiency and maximizes the output power of the PEMFC.

B. CASE 2: CHANGING MEMBRANE WATER CONTENT

In this case study, the four considered MPPT methods are tested at changing membrane water content, while keeping the operating temperature constant at 343 K. The membrane water content has been stepped several times to validate the response of the various MPPT methods as shown in Fig. 14. Fig. 15 shows the output power of the PEMFCs. Although, the four techniques can achieve MPPT, they have different overshoots/undershoots in addition to tracking time. It can be seen that the proposed OFLC MPPT method has the best performance compared to the other MPPT method for all scenarios. The proposed OFLC MPPT method achieves fast tracking with minimized power overshoots/undershoots. Whereas, the INC and P&O methods show slower tracking

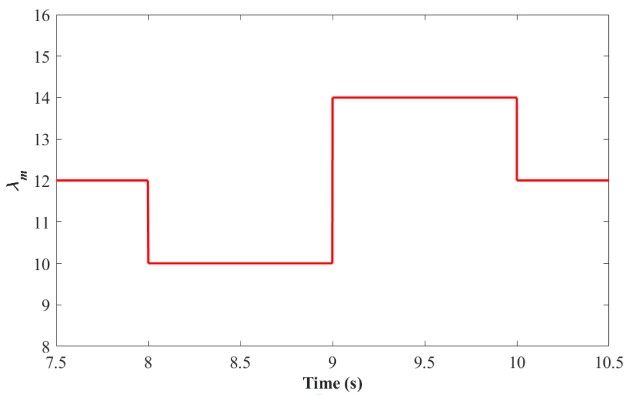

FIGURE 14. The considered changes in the membrane flow rate for case 2.

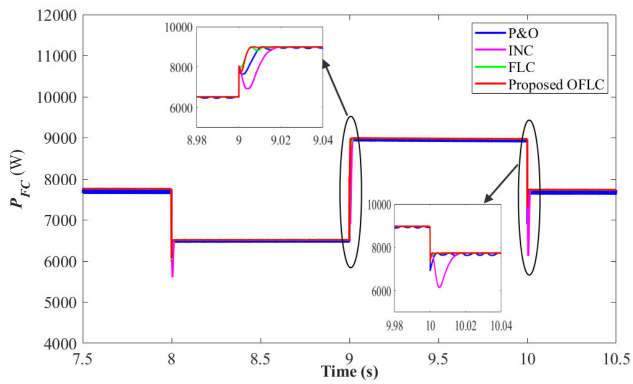

FIGURE 15. Performance comparison of the output power of the fuel cell for various MPPT methods at case 2.

of the MPPT. Moreover, the power ripple at steady state is minimum for the proposed OFLC method.

The performance of the outputted voltage of the PEMFC is compared in Fig. 16. It can be seen that the P&O MPPT method has the highest steady state fluctuations of the outputted PEMFC voltage waveform. Whereas, the proposed OFLC MPPT has small fluctuations in the outputted voltage waveform. Moreover, the overshoots/undershoots and the settling time is minimum for the proposed OFLC MPPT compared to the response of the other MPPT methods. The proposed OFLC MPPT method performs fast tracking of the

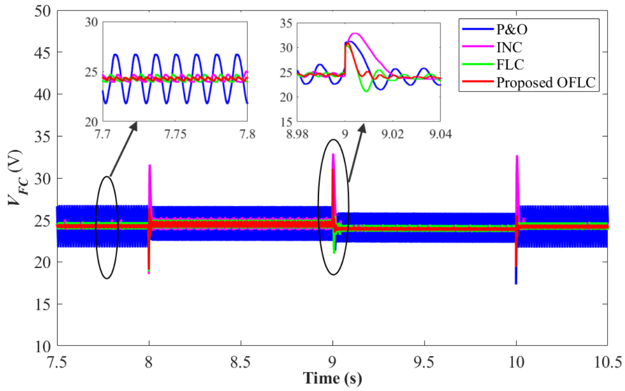

FIGURE 16. Performance comparison of the output voltage of the fuel cell for various MPPT methods at case 2.

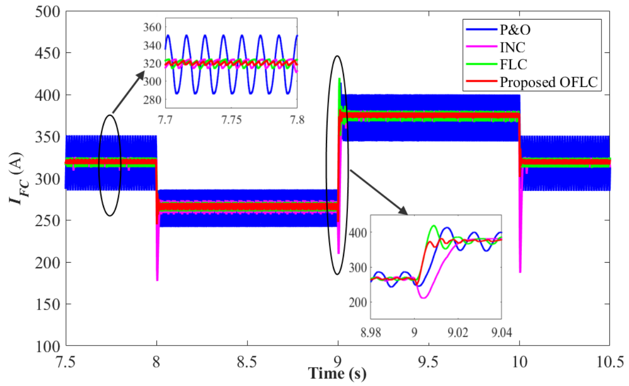

FIGURE 17. Performance comparison of the output current of the fuel cell for various MPPT methods at case 2.

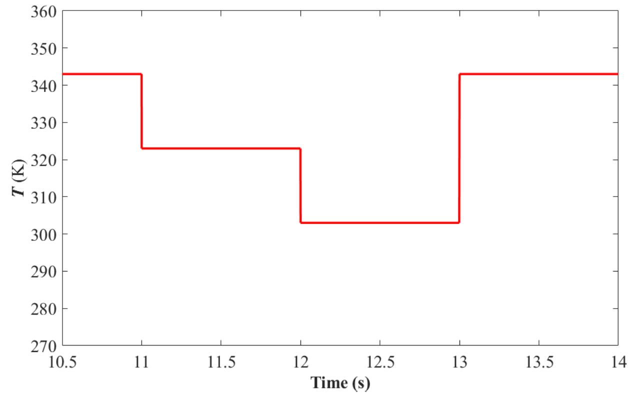

FIGURE 18. The considered changes in the fuel cell temperature for case 3.

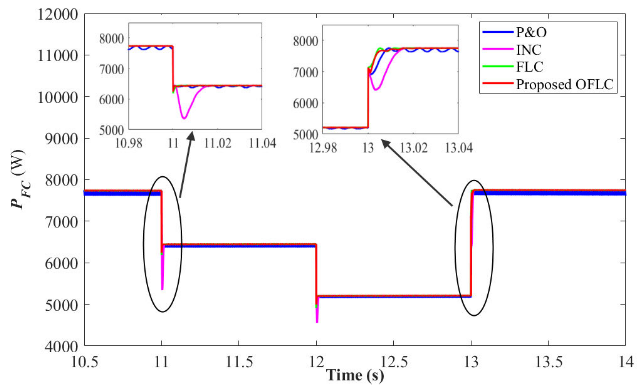

FIGURE 19. Performance comparison of the output power of the fuel cell for various MPPT methods at case 3.

MPP voltage of the PEMFC compared to the together three MPPT methods.

From another side, the output current of the PEMFC is compared for the considered MPPT methods and the results are shown in Fig. 17. It is clear that the proposed OFLC MPPT method has minimized PEMFC output current ripple compared to the high current ripple of the P&O MPPT method. From the overshoot/undershoot criteria, the proposed OFLC MPPT method provides reduced values compared to the other methods. It can also be seen that traditional MPPT methods compromise the tracking speed and the overshoot/undershoot values. However, the proposed OFLC MPPT is adaptive without compromising the settling time and/or overshoot/undershoot behavior.

C. CASE 3: CHANGING TEMPERATURE

Fig. 18 shows the tested scenarios of changing the temperature at membrane water content of 12. In this scenario, the several step-up and step-down changes of the temperature are performed to validate the performance of the proposed OFLC MPPT method. The outputted power waveforms for the considered MPPT methods are compared at both the steady state and transient response in Fig. 19. The P&O method has the highest steady state ripples of the outputted power waveform. In addition, the INC MPPT method possesses the highest transient overshoot/undershoot performance in addition to the longest settling time. Whereas, the MPPT response of PEMFC output waveforms are optimized using the proposed OFLC MPPT method. This in turn leads to improved efficiency of the PEMFC operation in addition to maximizing the outputted power from the cell. Moreover, the proposed OFLC MPPT method perform proper tracking with minimized ripples of the outputted power from the PEMFC.

In addition, Fig. 20 compared the PEMFC output voltage waveforms of the considered MPPT methods. All the methods are compared for the the steady state voltage ripples and transient response performance. The zoomed-in results shows the reduced PEMFC output voltage ripples compared to the widely employed P&O MPPT method, which possesses the highest steady state ripples of the outputted voltage waveform. In addition, the INC MPPT method possesses the highest transient overshoot/undershoot performance in addition to the longest settling time. The classical FLC MPPT method has multiple overshoot/undershoot response. Whereas, the new proposed OFLC MPPT method achieves enhanced tracking of the MPP voltage reference.

The outputted current waveforms are compared at both the steady state and transient response in Fig. 21. From the steady state response, the proposed OFLC MPPT method

TABLE 3. Performance comparison between MPPT methods.

Criteria	MPPT Methods			
	P&O	INC	FLC	Proposed OFLC
Reference	Ref. [20]	Ref. [24] and Ref. [22]	Ref. [34] and Ref. [38]	Proposed
Step Size	Fixed	Variable	Variable	Variable
Degree-of-freedom	Very Small	Very Small	Medium	Very High
Performance	Non-Optimized	Non-Optimized	Non-Optimized	Optimized
FC Output Fluctuations	High	High	Medium	Small
Tracking Time	High	Very High	Medium	Small

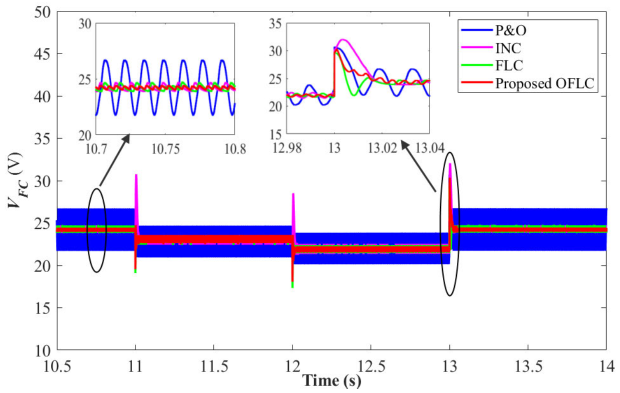

FIGURE 20. Performance comparison of the output voltage of the fuel cell for various MPPT methods at case 3.

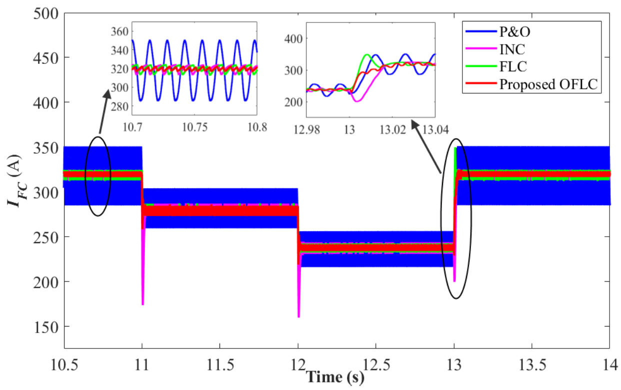

FIGURE 21. Performance comparison of the output current of the fuel cell for various MPPT methods at case 3.

is advantageous at achieving small output current ripples, whereas the classical P&O method has the highest steady state ripple in the PEMFC output current waveform. In addition, highest transient overshoot/undershoot performance is clear in the INC MPPT method response. From another side, the settling time of the new proposed method is small compared to the other three MPPT methods. This in turn validates the superior performance of the new proposed MPPT method for all the tested scenarios.

VI. DISCUSSION AND PERFORMANCE COMPARISON

Based on the aforementioned comparative results, Table 3 summarizes the performance comparison between the proposed OFLC method and the featured methods in the literature. The P&O MPPT method employs a fixed step size for the MPPT tracking. Therefore, only the step size can be optimized and it has very small degree-of-freedom. In addition, the results show that the P&O method has high fluctuation in the outputted power, voltage, and current of the FC. In addition, it possesses a high tracking time for the MPP. Whereas, the INC, FLC, and OFLC methods employ variable step size for tracking the MPP of the PEMFC. However, the proposed OFLC method has very high degree-of-freedom for optimizing the various parameters of the classical FLC MPPT method. Moreover, the proposed OFLC method achieves the fastest tracking response with the lowest tracking time.

VII. CONCLUSION

In this paper, a new optimized FLC (OFLC) based MPPT controller is presented for PEMFCs. The PEMFCs suffer from their nonlinear behavior and thence they have unique MPP. The high performance DEOA is employed in the proposed method for determining the various optimum variables of the proposed OFLC MPPT method. The proposed method has superior high degree of freedom degree-of-freedom compared to the other existing MPPT methods. The degree-of-freedom in the proposed OFLC MPPT method is achieved through optimizing the various settings for the membership functions (MFs) of the input and output variables. The proposed OFLC MPPT method has been validated and compared to the existing MPPT method in the literature. The results show that the proposed method can achieve accurate and fast tracking of optimal power point of the PEMFCs.The proposed method has achieved lower ripples and fluctuations in the output waveforms of the PEMFC. Moreover, fast with lower overshoot/undershoot response are obtained by applying the proposed OFLC MPPT method at step changes in the temperature and/or membrane water content.

REFERENCES

[1] E. M. Ahmed, M. Aly, A. Elmelegi, A. G. Alharbi, and Z. M. Ali, "Multifunctional distributed MPPT controller for 3P4W grid-connected PV systems in distribution network with unbalanced loads," *Energies*, vol. 12, no. 24, p. 4799, Dec. 2019.

[2] A. Elmelegi, M. Aly, E. M. Ahmed, and A. G. Alharbi, "A simplified phase-shift PWM-based feedforward distributed MPPT method for grid-connected cascaded PV inverters," *Sol. Energy*, vol. 187, pp. 1–12, Jul. 2019.

[3] A. Rezvani and M. Gandomkar, "Modeling and control of grid connected intelligent hybrid photovoltaic system using new hybrid fuzzy-neural method," *Sol. Energy*, vol. 127, pp. 1–18, Apr. 2016.

[4] N. Priyadarshi, M. S. Bhaskar, S. Padmanaban, F. Blaabjerg, and F. Azam, "New CUK–SEPIC converter based photovoltaic power system with hybrid GSA–PSO algorithm employing MPPT for water pumping applications," *IET Power Electron.*, early access, Jan. 2020.

[5] Y. Li, S. Q. Mohammed, G. S. Nariman, N. Aljojo, A. Rezvani, and S. Dadfar, "Energy management of microgrid considering renewable energy sources and electric vehicles using the backtracking search optimization algorithm," *J. Energy Resour. Technol.*, vol. 142, no. 5, pp. 1–18, Feb. 2020.

[6] N. Priyadarshi, S. Padmanaban, M. S. Bhaskar, F. Blaabjerg, J. B. Holm-Nielsen, F. Azam, and A. K. Sharma, "A hybrid photovoltaic-fuel cell-based single-stage grid integration with Lyapunov control scheme," *IEEE Syst. J.*, vol. 14, no. 3, pp. 3334–3342, Sep. 2020.

[7] M. H. Mostafa, S. H. E. Abdel Aleem, S. G. Ali, Z. M. Ali, and A. Y. Abdelaziz, "Techno-economic assessment of energy storage systems using annualized life cycle cost of storage (LCCOS) and levelized cost of energy (LCOE) metrics," *J. Energy Storage*, vol. 29, Jun. 2020, Art. no. 101345.

[8] W. Chen, Z. Shao, K. Wakil, N. Aljojo, S. Samad, and A. Rezvani, "An efficient day-ahead cost-based generation scheduling of a multi-supply microgrid using a modified krill herd algorithm," *J. Cleaner Prod.*, vol. 272, Nov. 2020, Art. no. 122364.

[9] S. M. Said, M. Aly, B. Hartmann, A. G. Alharbi, and E. M. Ahmed, "SMES-based fuzzy logic approach for enhancing the reliability of microgrids equipped with PV generators," *IEEE Access*, vol. 7, pp. 92059–92069, 2019.

[10] H. G. Lee, G.-G. Kim, B. G. Bhang, D. K. Kim, N. Park, and H.-K. Ahn, "Design algorithm for optimum capacity of ESS connected with PVs under the RPS program," *IEEE Access*, vol. 6, pp. 45899–45906, 2018.

[11] L. Luo, S. S. Abdulkareem, A. Rezvani, M. R. Miveh, S. Samad, N. Aljojo, and M. Pazhoohesh, "Optimal scheduling of a renewable based microgrid considering photovoltaic system and battery energy storage under uncertainty," *J. Energy Storage*, vol. 28, Apr. 2020, Art. no. 101306.

[12] M. M. Alhaider, E. M. Ahmed, M. Aly, H. A. Serhan, E. A. Mohamed, and Z. M. Ali, "New temperature-compensated multi-step constant-current charging method for reliable operation of battery energy storage systems," *IEEE Access*, vol. 8, pp. 27961–27972, 2020.

[13] B. Wang, D. Zhao, W. Li, Z. Wang, Y. Huang, Y. You, and S. Becker, "Current technologies and challenges of applying fuel cell hybrid propulsion systems in unmanned aerial vehicles," *Prog. Aerosp. Sci.*, vol. 116, Jul. 2020, Art. no. 100620.

[14] X. Lü, P. Wang, L. Meng, and C. Chen, "Energy optimization of logistics transport vehicle driven by fuel cell hybrid power system," *Energy Convers. Manage.*, vol. 199, Nov. 2019, Art. no. 111887.

[15] H. Beirami, A. Z. Shabestari, and M. M. Zerafat, "Optimal PID plus fuzzy controller design for a PEM fuel cell air feed system using the self-adaptive differential evolution algorithm," *Int. J. Hydrogen Energy*, vol. 40, no. 30, pp. 9422–9434, Aug. 2015.

[16] B. Yang, J. Wang, L. Yu, H. Shu, T. Yu, X. Zhang, W. Yao, and L. Sun, "A critical survey on proton exchange membrane fuel cell parameter estimation using meta-heuristic algorithms," *J. Cleaner Prod.*, vol. 265, Aug. 2020, Art. no. 121660.

[17] N. Benyahia, H. Denoun, A. Badji, M. Zaouia, T. Rekioua, N. Benamrouche, and D. Rekioua, "MPPT controller for an interleaved boost DC–DC converter used in fuel cell electric vehicles," *Int. J. Hydrogen Energy*, vol. 39, no. 27, pp. 15196–15205, Sep. 2014.

[18] Y. Wu, Y. Huangfu, R. Ma, A. Ravey, and D. Chrenko, "A strong robust DC-DC converter of all-digital high-order sliding mode control for fuel cell power applications," *J. Power Sources*, vol. 413, pp. 222–232, Feb. 2019.

[19] S. Samal, M. Ramana, and P. K. Barik, "Modeling and simulation of interleaved boost converter with MPPT for fuel cell application," in *Proc. Technol. Smart-City Energy Secur. Power (ICSESP)*, Mar. 2018, pp. 1–5.

[20] N. Naseri, S. E. Hani, A. Aghmadi, K. E. Harouri, M. S. Heyine, and H. Mediouni, "Proton exchange membrane fuel cell modelling and power control by P&O algorithm," in *Proc. 6th Int. Renew. Sustain. Energy Conf. (IRSEC)*, Dec. 2018, pp. 1–5.

[21] H. Rezk and A. Fathy, "Performance improvement of PEM fuel cell using variable step-size incremental resistance MPPT technique," *Sustainability*, vol. 12, no. 14, p. 5601, Jul. 2020.

[22] A. Peer Mohamed, K. R. M. Vijaya Chandrakala, and S. Saravanan, "Comparative study of maximum power point tracking techniques for fuel cell powered electric vehicle," *IOP Conf., Mater. Sci. Eng.*, vol. 577, Dec. 2019, Art. no. 012031.

[23] V. Karthikeyan, P. V. Das, and F. Blaabjerg, "Implementation of MPPT control in fuel cell fed high step up ratio DC-DC converter," in *Proc. 2nd IEEE Int. Conf. Power Electron., Intell. Control Energy Syst. (ICPEICES)*, Oct. 2018, pp. 689–693.

[24] A. Harrag and S. Messalti, "Variable step size IC MPPT controller for PEMFC power system improving static and dynamic performances," *Fuel Cells*, vol. 17, no. 6, pp. 816–824, Nov. 2017.

[25] P.-Y. Chen, K.-N. Yu, H.-T. Yau, J.-T. Li, and C.-K. Liao, "A novel variable step size fractional order incremental conductance algorithm to maximize power tracking of fuel cells," *Appl. Math. Model.*, vol. 45, pp. 1067–1075, May 2017.

[26] K. Jyotheeswara Reddy and N. Sudhakar, "High voltage gain interleaved boost converter with neural network based MPPT controller for fuel cell based electric vehicle applications," *IEEE Access*, vol. 6, pp. 3899–3908, 2018.

[27] S. Padmanaban, N. Priyadarshi, M. S. Bhaskar, J. B. Holm-Nielsen, E. Hossain, and F. Azam, "A hybrid photovoltaic-fuel cell for grid integration with Jaya-based maximum power point tracking: Experimental performance evaluation," *IEEE Access*, vol. 7, pp. 82978–82990, 2019.

[28] S. Ahmadi, S. Abdi, and M. Kakavand, "Maximum power point tracking of a proton exchange membrane fuel cell system using PSO-PID controller," *Int. J. Hydrogen Energy*, vol. 42, no. 32, pp. 20430–20443, Aug. 2017.

[29] A. Fathy, M. A. Abdelkareem, A. G. Olabi, and H. Rezk, "A novel strategy based on salp swarm algorithm for extracting the maximum power of proton exchange membrane fuel cell," *Int. J. Hydrogen Energy*, Mar. 2020.

[30] K. P. S. Rana, V. Kumar, N. Sehgal, and S. George, "A novel dPdI feedback based control scheme using GWO tuned PID controller for efficient MPPT of PEM fuel cell," *ISA Trans.*, vol. 93, pp. 312–324, Oct. 2019.

[31] Shashikant and B. Shaw, "Comparison of SCA-optimized PID and P&O-based MPPT for an off-grid fuel cell system," in *Soft Computing in Data Analytics*. Singapore: Springer, Aug. 2018, pp. 51–58.

[32] S. Kumar and B. Shaw, "Design of off-grid fuel cell by implementing ALO optimized PID-based MPPT controller," in *Soft Computing in Data Analytics*. Singapore: Springer, Aug. 2018, pp. 83–93.

[33] H. Rezk, M. Aly, M. Al-Dhaifallah, and M. Shoyama, "Design and hardware implementation of new adaptive fuzzy logic-based MPPT control method for photovoltaic applications," *IEEE Access*, vol. 7, pp. 106427–106438, 2019.

[34] A. Harrag and S. Messalti, "How fuzzy logic can improve PEM fuel cell MPPT performances?" *Int. J. Hydrogen Energy*, vol. 43, no. 1, pp. 537–550, Jan. 2018.

[35] N. Harrabi, M. Souissi, A. Aitouche, and M. Chaabane, "Modeling and control of photovoltaic and fuel cell based alternative power systems," *Int. J. Hydrogen Energy*, vol. 43, no. 25, pp. 11442–11451, Jun. 2018.

[36] D. N. Luta and A. K. Raji, "Comparing fuzzy rule-based MPPT techniques for fuel cell stack applications," *Energy Procedia*, vol. 156, pp. 177–182, Jan. 2019.

[37] N. Priyadarshi, A. K. Sharma, and F. Azam, "A hybrid firefly-asymmetrical fuzzy logic controller based MPPT for PV-wind-fuel grid integration," *Int. J. Renew. Energy Res.*, vol. 7, no. 4, pp. 1546–1560, 2017.

[38] D. Luta and A. Raji, "Fuzzy rule-based and particle swarm optimisation MPPT techniques for a fuel cell stack," *Energies*, vol. 12, no. 5, p. 936, Mar. 2019.

[39] N. Priyadarshi, S. Padmanaban, M. Sagar Bhaskar, F. Blaabjerg, and A. Sharma, "Fuzzy SVPWM-based inverter control realisation of grid integrated photovoltaic-wind system with fuzzy particle swarm optimisation maximum power point tracking algorithm for a grid-connected PV/wind power generation system: Hardware implementation," *IET Electr. Power Appl.*, vol. 12, no. 7, pp. 962–971, Aug. 2018.

[40] S. Padmanaban, N. Priyadarshi, M. S. Bhaskar, J. B. Holm-Nielsen, E. Hossain, and F. Azam, "A hybrid photovoltaic-fuel cell for grid integration with jaya-based maximum power point tracking: Experimental performance evaluation," *IEEE Access*, vol. 7, pp. 82978–82990, 2019.

[41] S. Padmanaban, N. Priyadarshi, J. B. Holm-Nielsen, M. S. Bhaskar, F. Azam, A. K. Sharma, and E. Hossain, "A novel modified sine-cosine optimized MPPT algorithm for grid integrated PV system under real operating conditions," *IEEE Access*, vol. 7, pp. 10467–10477, 2019.

[42] Y. Li, S. Samad, F. W. Ahmed, S. S. Abdulkareem, S. Hao, and A. Rezvani, "Analysis and enhancement of PV efficiency with hybrid MSFLA–FLC MPPT method under different environmental conditions," *J. Cleaner Prod.*, vol. 271, Oct. 2020, Art. no. 122195.

[43] X. Ge, F. W. Ahmed, A. Rezvani, N. Aljojo, S. Samad, and L. K. Foong, "Implementation of a novel hybrid BAT-fuzzy controller based MPPT for grid-connected PV-battery system," *Control Eng. Pract.*, vol. 98, May 2020, Art. no. 104380.

[44] N. Priyadarshi, S. Padmanaban, P. Kiran Maroti, and A. Sharma, "An extensive practical investigation of FPSO-based MPPT for grid integrated PV system under variable operating conditions with anti-islanding protection," *IEEE Syst. J.*, vol. 13, no. 2, pp. 1861–1871, Jun. 2019.

[45] A. Raj and P. Lekhaj, "An ANFIS based MPPT controller for fuel cell powered induction motor drive," in *Proc. Int. Conf. Smart Grid Clean Energy Technol. (ICSGCE)*, May 2018, pp. 201–205.

[46] N. Priyadarshi, S. Padmanaban, J. B. Holm-Nielsen, F. Blaabjerg, and M. S. Bhaskar, "An experimental estimation of hybrid ANFIS–PSO-based MPPT for PV grid integration under fluctuating sun irradiance," *IEEE Syst. J.*, vol. 14, no. 1, pp. 1218–1229, Mar. 2020.

[47] S. Padmanaban, N. Priyadarshi, M. Sagar Bhaskar, J. B. Holm-Nielsen, V. K. Ramachandaramurthy, and E. Hossain, "A hybrid ANFIS-ABC based MPPT controller for PV system with anti-islanding grid protection: Experimental realization," *IEEE Access*, vol. 7, pp. 103377–103389, 2019.

[48] N. Priyadarshi, S. Padmanaban, L. Mihet-Popa, F. Blaabjerg, and F. Azam, "Maximum power point tracking for brushless DC motor-driven photovoltaic pumping systems using a hybrid ANFIS-FLOWER pollination optimization algorithm," *Energies*, vol. 11, no. 5, p. 1067, Apr. 2018.

[49] K. J. Reddy and N. Sudhakar, "ANFIS-MPPT control algorithm for a PEMFC system used in electric vehicle applications," *Int. J. Hydrogen Energy*, vol. 44, no. 29, pp. 15355–15369, Jun. 2019.

[50] A. Harrag and H. Bahri, "Novel neural network IC-based variable step size fuel cell MPPT controller," *Int. J. Hydrogen Energy*, vol. 42, no. 5, pp. 3549–3563, Feb. 2017.

[51] K. P. S. Rana, V. Kumar, N. Sehgal, and S. George, "A novel dPdI feedback based control scheme using GWO tuned PID controller for efficient MPPT of PEM fuel cell," *ISA Trans.*, vol. 93, pp. 312–324, Oct. 2019.

[52] O. Guenounou, B. Dahhou, and F. Chabour, "Adaptive fuzzy controller based MPPT for photovoltaic systems," *Energy Convers. Manage.*, vol. 78, pp. 843–850, Feb. 2014.

[53] M. Dehghani, M. Taghipour, G. B. Gharehpetian, and M. Abedi, "Optimized fuzzy controller for MPPT of grid-connected PV systems in rapidly changing atmospheric conditions," *J. Mod. Power Syst. Clean Energy*, early access, May 2020.

[54] S. Das, S. S. Mullick, and P. N. Suganthan, "Recent advances in differential evolution—An updated survey," *Swarm Evol. Comput.*, vol. 27, pp. 1–30, Apr. 2016.

MOKHTAR ALY (Member, IEEE) received the B.Sc. and M.Sc. degrees in electrical engineering from Aswan University, Aswan, Egypt, in 2007 and 2012, respectively, and the Ph.D. degree from the Department of Electrical Engineering, Faculty of Information Science and Electrical Engineering, Kyushu University, Japan, in 2017.

In 2008, he joined the Department of Electrical Engineering, Aswan University, as an Assistant Lecturer, where he has been an Assistant Professor with the Faculty of Engineering, since 2017. He is currently a Postdoctoral Researcher with the Solar Energy Research Center (SERC-Chile), Universidad Técnica Federico Santa María, Chile. His current research interests include reliability of power electronics systems especially in renewable energy applications, multilevel inverters, fault tolerant control, electric vehicles, and light emitting diode (LED) lamp drivers. He is a member in the IEEE Power Electronics Society (PELS), the IEEE Industrial Electronics Society (IES), and the IEEE Power and Energy Society (PES).

HEGAZY REZK received the B.Eng. and M.Eng. degrees in electrical engineering from Minia University, Egypt, in 2001 and 2006, respectively, and the Ph.D. degree from the Moscow Power Engineering Institute, Moscow. He was a Postdoctoral Research Fellow of mechanical engineering with the Moscow State University, in 2014. He was a Visiting Researcher with Kyushu University, Japan, in 2015. He is currently an Associate Professor with the Department of Electrical Engineering, Collage of Engineering at Wadi Addwaser, Prince Sattam Bin Abdulaziz University, Saudi Arabia. He has authored more than 100 technical articles. His current research interests include renewable and sustainable energy, energy management, energy efficiency modern optimization algorithms, and modeling based on artificial intelligence.